10 March 1995

ELSEVIER

Chemical Physics Letters 234 (1995) 281–288

CHEMICAL PHYSICS LETTERS

Ponderomotive effects in zero kinetic energy photoelectron spectroscopy with intense femtosecond pulses

A. Zavriyev, Ingo Fischer, D.M. Villeneuve, Albert Stolow

Steacie Institute for Molecular Sciences, National Research Council, Ottawa, Ontario, Canada K1A 0R6

Received 14 December 1994

Abstract

Zero kinetic energy photoelectron (ZEKE) spectroscopy may be an interesting technique for monitoring the time evolution of state selected atomic products in ultrafast pump–probe experiments. We investigate here the effects of laser intensity by studying three-photon non-resonant ZEKE spectra of atomic xenon at the first ionization threshold with tunable femtosecond UV pulses. High intensity introduces a new broadening due to ponderomotive effects in the ZEKE spectrum. It is demonstrated that a three-photon ZEKE spectrum can be recorded at intensities where the broadening due to these ponderomotive effects (i.e. the ac Stark shift for high-n Rydberg states) is small in comparison with the effective laser bandwidth.

1. Introduction

The advent of femtosecond pump–probe spectroscopy has allowed researchers to explore new approaches to the study of gas phase reaction dynamics [1]. The time evolution of both the initial states [2] and products [1,3,4] has been monitored by a variety of techniques. Examples involving detection of photons are direct absorption [4], laser-induced fluorescence [1,2,5] and stimulated emission pumping [6]. Examples involving the detection of ions are given in Refs. [1,7–10]. The advantages of ion detection are the possibility of mass analysis and the high detection sensitivity. Ion detection, however, does not readily permit determination of the internal states of the product. By contrast, fluorescence may be dispersed in a monochromator in order to improve final state selectivity. An analogous 'dispersed' technique for charged particle detection is photoelectron spectroscopy: The electrons can be further analyzed as to their kinetic energy, described for example in Refs. [11,12]. One experimental problem associated with ion and electron time-of-flight detection is the occurrence of background signals due to ionization from pump or probe laser alone. A technique does exist, however, which circumvents this problem, namely zero kinetic energy (ZEKE) spectroscopy [13,14].

The pulsed field ionization of Rydberg states, termed ZEKE, is based on the excitation of molecules or atoms to very high lying Rydberg states a few wavenumbers below a certain final state of the ion. These are then detected by applying a pulsed electric field after a delay time on the order of several 100 ns. The technique is background-free in the sense that only the proper combination of pump and probe photons produce a Rydberg state. All other combinations might well produce kinetic electrons (due to multiphoton ionization) but these leave the interaction region during the delay time and are not de-

Elsevier Science B.V.
SSDI 0009-2614(95)00049-6

tected. ZEKE spectroscopy has been applied to picosecond pump–probe experiments with great success [15]. The use of ZEKE detection in femtosecond experiments has been demonstrated at a fixed probe wavelength on the Na_3 system [16], and, with tunable pulses, on the wavepacket dynamics of the I_2 B state [17]. We consider now the applicability of ZEKE spectroscopy in monitoring the time evolution of atomic products in a femtosecond pump–probe experiment. The reason for doing so is the possibility for state selective, background-free detection. In such an experiment one would 'recognize' the atom by its ionization potential (IP) rather than its charge-to-mass ratio. The IP of many atoms, however, lies in the 12 eV range, requiring the use of vacuum ultraviolet (VUV) radiation. Although ZEKE spectroscopy with nanosecond VUV-pulses proved to be quite successful [18–20], the difficulties associated with generating ≈ 100 fs VUV pulses [21–23] lead us to consider other possibilities.

The inherent high peak power of femtosecond pulses suggests the idea of multiphoton non-resonant ZEKE detection of atoms. To excite an atom with an IP of 12 eV to its ionization threshold requires three photons with a wavelength around 300 nm, a relatively accessible region. Two-photon non-resonant ZEKE spectroscopy using nanosecond pulses has been applied to several molecular systems [24]. The extension to three-photon non-resonant processes seems obvious considering the intensity of amplified femtosecond pulses. High laser intensity, however, can introduce other often undesirable effects. The purpose of this Letter is to investigate the effects of laser intensity on the *spectroscopic* detection of atoms in the gas phase using three-photon non-resonant ZEKE-spectroscopy.

The probability for a non-resonant n-photon absorption process, P^n, can be described as

$$P^n \sim I^n t, \tag{1}$$

where I is the intensity of the laser light and t the duration of the pulse. Due to the short pulse duration used in time-resolved experiments, one is forced to use high laser intensities in order to obtain a significant transition probability. As is well known in atomic physics the influence of the laser field strength on atomic ionization is non-negligible [25]. It introduces the so-called ponderomotive potential, U_p, which acts in a similar way on free electrons and Rydberg states. It shifts the ionization potential to higher energies and introduces an additional broadening of the atomic states [26,27]. It is the ac Stark shift for free electrons and high-n Rydberg states. In a classical description, U_p is given by the 'wiggling' energy of a free electron in the laser field,

$$U_p = e^2 E_0^2 / 4 m_e \omega^2, \tag{2}$$

where E_0 is the electric field of the laser, m_e is the mass of the electron and ω is the angular frequency of the incident light. A rule of thumb is that the ponderomotive shift is approximately 10 meV per TW/cm^2 at 330 nm. U_p scales linearly with the laser intensity and quadratically with the wavelength. For a 100 fs pulse, even under moderate focusing conditions ($f/40$ optics), 1 TW/cm^2 at 330 nm corresponds to an energy of only ≈ 1 μJ. Consequently, the ponderomotive shift becomes important in ionization experiments using sub-picosecond laser pulses. If much higher intensities are used, the corresponding broadening of the ZEKE spectrum will become so large that the state selectivity of the method is lost.

In order to explore the influence of the laser field strength on the ZEKE spectrum we studied three-photon ZEKE spectroscopy of atomic xenon. The xenon ionization energy of 12.130 eV [28] is a typical value for non-metallic atoms and many diatomic molecules. Thus the results can easily be extended to other species. As the one- and two-photon energies employed in the experiment are several electron volt away from excited electronic states of the Xe atom, the three-photon process is truly non-resonant.

In the following sections we will address the central question of this Letter. Is it possible to record a three-photon ZEKE spectrum at laser intensities where the ponderomotive shift is smaller than the laser bandwidth? The concepts applied in the current work are familiar to those working in the field of atomic physics. Related work was done by Landen et al. [29] who examined the ac Stark shift in three-photon transitions to high-lying states of krypton. O'Brian et al. demonstrated the near-ponderomotive behavior of the ac Stark-shift in Rydberg states of xenon [30], using two-colour three-photon ionization. We hope to point out the important consequences of

high intensity for time-resolved, as well as for very high-resolution nanosecond ZEKE experiments that emerge from these concepts.

2. Experimental

The laser system used in the present experiment is depicted in Fig. 1. It consists of a passively mode-locked tunable femtosecond dye laser (Coherent Satori) synchronously pumped by the second harmonic of a mode-locked Nd:YAG laser (Coherent Antares). For the present study the broad bandwidth of the laser was spectrally filtered and selected as the seed pulse for a five-stage prism dye cell amplifier chain [31], pumped by the second harmonic of a Q-switched Nd:YAG laser (Lumonics H8400). The amplified pulses were not recompressed. In order to relate the measurable laser pulse *energy* to the *intensity* the spatial profile of the laser at the focus must be known. Therefore, the amplified beam was spatially filtered. We obtained a maximum pulse energy of 200 μJ in 480 fs at a bandwidth of 3 nm (80 cm^{-1}) after the spatial filter. The central wavelength and bandwidth of the amplified pulse were determined using an optical multichannel analyzer which was calibrated by means of the 632.8 nm HeNe laser line and the 532 nm light from the Nd:YAG laser. The pulse duration was determined in a single-shot autocorrelator.

The collimated light was doubled in a 3 mm KDP crystal yielding a maximum UV energy of 3 μJ. Due to the overly long crystal length, we obtained a 900 fs UV pulse with a nearly square temporal profile. Thus the calculation of intensities is significantly simplified and the comparison of the experiments with a simple model of ponderomotive shifts facilitated. (The increase in pulse duration is not important for this one-laser experiment.) It is, however, important that the pulse duration was constant for each measured shot. This was ensured by measuring the autocorrelation ratio (ACR) for each laser pulse, as explained in the following: At a given pulse duration the intensity of the UV light depends only on the pulse energy. By measuring the ratio of the second harmonic energy to the fundamental energy squared (i.e. the ACR), as shown in Fig. 1, we were able to filter our data. For a constant pulse duration the ACR remains fixed. Typically, we use a 10% acceptance bandwidth on the ACR. Laser pulses

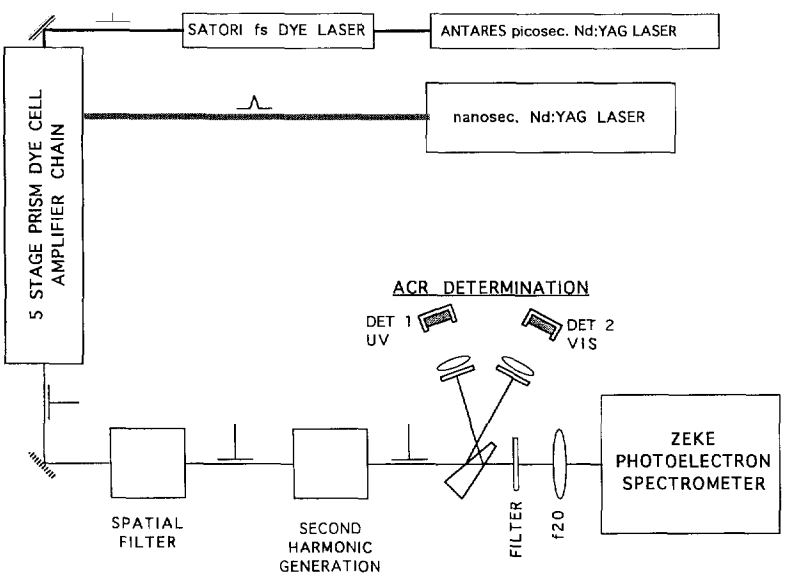

Fig. 1. Depiction of the laser system employed in the experiment. The output of a femtosecond linear dye laser is amplified, spatially filtered and frequency doubled. Reflections from a wedge of both the fundamental and the second harmonic were recorded on the photodiodes DET 1 and 2, in order to monitor the power and control the duration of the pulse through the ACR (see text)

outside this range were rejected. The procedure described above was utilized in earlier experiments [32].

The UV light was focused by means of $F/20$ optics into a pulsed jet of pure xenon (backing pressure 330 Torr). No clusters were observed at the pulsed valve time-delay used in the experiment. The vacuum chamber was equipped with a time-of flight spectrometer perpendicular to both the laser beam and the jet. As the drift tube was not magnetically shielded, a rather high extraction pulse of $\mathscr{E} = 240$ V/cm was applied to ensure high collection efficiency of the ZEKE electrons. During the delay time of 500 ns between the laser pulse and the extraction pulse, a 2 V/cm dc offset field was present in order to sweep the kinetic electrons out of the interaction region. The electrons were detected at a microchannel plate detector (MCP). The amplified signals from the MCP and the photodiodes were recorded by several boxcar integrators and transferred to a computer.

The energy of the UV light pulses fluctuated typically by a factor of 10 during the experiment. As the fluctuations are proportional to the intensity, and independent of the pulse duration, they were used to record the ZEKE signal at different intensities but fixed wavelength. The signals from the MCP were sorted into 10 intensity bins according to the signal

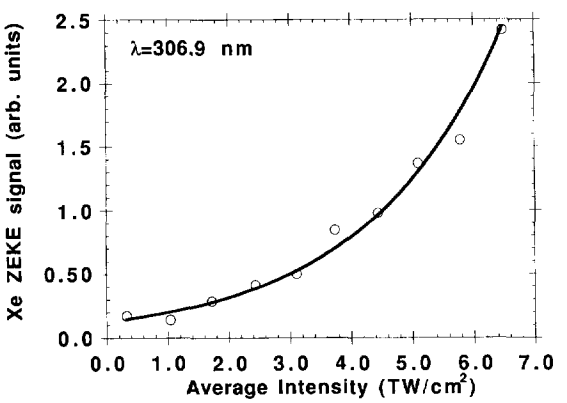

Fig. 2. Example least squares exponential fit of the experimental data at 306.9 nm. The values for the average laser intensities were calculated by means of formula (3). Similar curves were obtained at the other wavelengths. At selected intensities the values are read out from the fits in order to obtain the data points shown in Fig. 3.

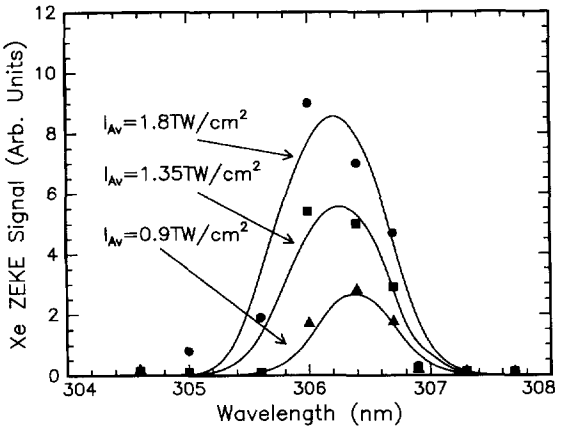

Fig. 3. The ZEKE spectrum of Xe at three selected intensities, 0.9, 1.35 and 1.8 TW/cm^2. The data points were obtained from a fit to the experimental data at each wavelength, as shown in Fig. 2. The curves as well as the values for the intensities are a result of calculations described in the text. A blue-shift of the peak maximum and a broadening of the peaks to the blue-side is observed with increasing intensity.

at the UV photodiode. Thus for a certain wavelength we obtained values for the ZEKE signal at 10 discrete values of the laser intensity. The laser would then be tuned to the next wavelength and the entire procedure was repeated.

3. Results and discussion

At each wavelength the three-photon ZEKE signal from atomic xenon was plotted as a function of the *average* laser intensity and least-squares fitted by an exponential interpolation curve. A typical example of such a curve is given in Fig. 2. At selected intensities on the curve, values of the ZEKE signal were read out and plotted as a function of the wavelength, yielding the data points in Fig. 3.

The values for the average intensity can be calculated according to the approximate formula

$$I_{\mathrm{av}} = \frac{P}{\pi(0.89F\lambda)^2\Delta t}, \qquad (3)$$

where P is the measured laser energy and the denominator gives the spot size of the laser focus times the pulse duration [33]. The values correspond to intensities averaged over the temporal and spatial

profile of the pulse. It should be noted that the relative average intensities can be determined very accurately with this formula, whereas the absolute values are probably uncertain to within a factor of 2, due to the fact that the beam profile (and thus the focal spot size) is not exactly known. At the lowest average intensity (0.5 TW/cm^2) the signal was indistinguishable from the noise level, showing that the laser intensity was too low to record a three-photon ZEKE signal in our spectrometer. However, at around 1 TW/cm^2 a signal was observed. At higher average intensity the signal is much more intense but a broadening of the peak to the blue-side is observed. The ponderomotive energy shifts the Rydberg states towards higher energy, broadening the peak to the blue-side only. For average intensities of 4 TW/cm^2 and higher, no points could be obtained in the bluest part of the spectrum because these wavelengths fall on the edge of the gain profile of the dye amplifier. For intensities greater than 6 TW/cm^2 with three-photon energies above the ionization threshold, a sudden increase in the signal intensity was observed. This is due to space charge effects which trap kinetic electrons and prevent them from leaving the interaction region. Those electrons are then detected together with the ZEKE electrons after the extraction pulse is applied. These 'false ZEKE' effects will be discussed in a forthcoming publication [34].

We will now concentrate on the intermediate intensity range between 1 and 2 TW/cm^2. The field-free ionization potential of Xe is 12.130 eV [28], which corresponds to 306.64 nm in three-photon ionization. Due to our extraction field of 240 V/cm we field-ionize all Rydberg-states prepared within 60 cm^{-1} below the ionization potential, assuming diabatic ionization [35]. The transition probability per energy interval close to the threshold is approximately constant (as discussed in a following paragraph) and the three-photon bandwidth is larger than the region of detected Rydberg states, as shown in Fig. 4. Furthermore, the field ionization probability per energy interval is equal for all Rydberg-states within the 60 cm^{-1} window and the influence of the comparatively small offset field of 2 V/cm is negligible. Thus, the maximum of the signal should be obtained when the overlap between the laser pulse spectrum and the region of detectable Rydberg states is maximized, that is at 30 cm^{-1} below threshold at a central wavelength of 306.74 nm on the three-photon scale. Any additional blue-shift of the peak maximum from this corrected ionization potential should be exclusively due to U_p, the ponderomotive potential.

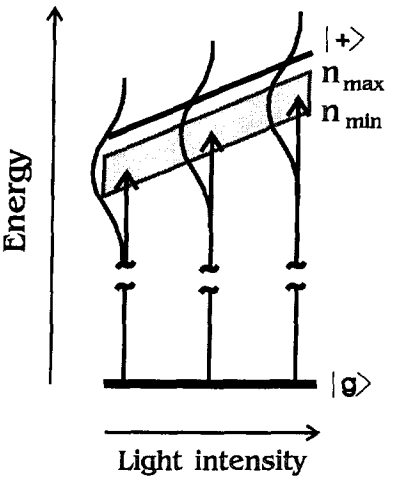

Fig. 4. The shaded area represents the region of Rydberg states that can be detected in our experiment: n_{max} being the highest Rydberg state that survives the dc offset field in our experiment; n_{min} being the lowest Rydberg state that is field-ionized with our 240 V/cm extraction field. |g⟩ symbolizes the ground state of xenon and |+⟩ the ground state of Xe^+. With increasing laser light intensity Rydberg states are shifted to higher energies. Thus the maximum of the signal is obtained at a shorter wavelength.

In order to compare our experimental results with a simple model, we must consider in more detail the spatial, temporal and spectral distribution of intensities within the laser focus. At a given point in the focus a xenon atom experiences a certain laser intensity. This intensity causes a ponderomotive shift of the Rydberg levels towards higher energies, as illustrated in Fig. 4. Therefore, the three-photon ZEKE spectrum is blue-shifted by an amount linearly proportional to the intensity felt by this atom. The probability, however, of exciting this atom depends nonlinearly (i.e. non-resonant three-photon excitation) on the laser intensity. Thus it is necessary to fit the data to the spatio-temporal distribution of the light intensities in the pulse in order to extract the ponderomotive shifts and the line broadening from the ZEKE spectrum.

Fig. 3 shows the predictions of a simple numerical model that we developed to compare with our experimental results. The data points in the figure represent the values of the signal at intensities read out from Fig. 2 and similar curves corresponding to different wavelengths. The smooth curves are the results of the calculations which are discussed below.

We considered a Gaussian spatial intensity distribution in the focus

$$I(\bar{r}, t) = I_0(t, z) \exp(-2r^2/w_0^2), \tag{4}$$

where w_0 is the focal waist, and $I_0(t)$ is the laser *peak* intensity which we assumed was a constant throughout the duration of the laser pulse (which was a very realistic assumption for our experimental conditions due to the broadening of the pulse to a square top profile in the long doubling crystal). We also modeled the laser radiation frequency spectrum by a Gaussian with the central frequency ν_0 and fwhm of $\delta\nu$. The probability of populating a Rydberg state with a principal quantum number n scales as n^{-3}, whereas the density of the states is proportional to n^3. This results in a uniform cross-section for three-photon excitation into Rydberg levels throughout the laser bandwidth. Therefore, in order to calculate the contribution from a particular spatial point, we first estimated the local shift of our detectable Rydberg bandwidth (equal to the local ponderomotive shift) and then evaluated the frequency–space overlap integral of our laser spectrum with the new (shifted) position of the detectable Rydberg bandwidth, as illustrated in Fig. 4.

The probability of finding an atom in a Rydberg state at the end of the laser interaction depends on the relative rates of two processes: (1) The non-resonant three-photon excitation of the atom from the ground state into the Rydberg state and (2) the subsequent ionization via absorption of additional photons. The photoexcitation rate is proportional to $\sigma_3 I^3$, where σ_3 is the three-photon excitation cross-section of the ground state and I is the local laser intensity. We considered only subsequent photoionization via one-photon absorption. With this assumption, the loss rate is proportional to $\sigma_1 I\rho(t)$, where σ_1 is the one-photon absorption cross-section of the Rydberg state and $\rho(t)$ is its population as a function of time.

If we neglect the depletion of the atomic ground state, the rate of change of the Rydberg population can then be written as

$$\frac{\mathrm{d}\rho}{\mathrm{d}t} = K_1\sigma_3 I^3 - K_2\sigma_1 I\rho(t), \tag{5}$$

where K_1 and K_2 are the proportionality coefficients. The Rydberg population after the laser interaction is then given by

$$\rho(\tau) = \frac{K_1\sigma_3 I^2}{K_2\sigma_1}\left[1 - \exp(-K_2\sigma_1 I\tau)\right], \tag{6}$$

where τ is the duration of the laser pulse. The high-lying Rydberg states that we experimentally detected were unlikely to ionize during our short laser pulse ($I\sigma_1\tau \ll 1$). Consequently, we could expand $\rho(\tau)$ in the power series of I,

$$\rho(\tau) = \sum_{i=3}^{\infty} (-1)^{i+1} C_i I^i. \tag{7}$$

For simplicity, we truncated the series at the term proportional to I^4 to get

$$\rho(\tau) = C_3 I^3 - C_4 I^4, \tag{8}$$

where C_3 and C_4 are non-negative coefficients. In order to simulate the experimental results we integrated over space and time, as well as the laser bandwidth (frequency),

$$R_{\text{total}} \propto \int \mathrm{d}^3 r \int_0^{\infty} \mathrm{d}\nu \times \left[C_3 I^3(\bar{r}, t, \nu) - C_4 I^4(\bar{r}, t, \nu)\right], \tag{9}$$

where R_{total} is the population left in the Rydberg states after the laser interaction. Two fitting parameters were used in the model: the ratio C_3/C_4 and the *peak* laser intensity. The intensity used to fit the data in Fig. 4 is in a good agreement with that calculated using Eq. (3).

The main source of error in the experiment is the determination of the central wavelength of the dye laser, which is only accurate to within ≈ 0.1 nm in the UV. This corresponds to error bars of ≈ 30 cm^{-1}. The halfwidths of the three fit curves are 250 cm^{-1} (0.9 $\mathrm{TW/cm^2}$), 300 cm^{-1} (1.75 $\mathrm{TW/cm^2}$) and 340 cm^{-1} (1.8 $\mathrm{TW/cm^2}$) on a three-photon scale. This has to be compared with a three-photon bandwidth of ≈ 200 cm^{-1} and a broadening of ≈ 60 cm^{-1} due to the dc Stark effect of our extrac-

tion pulse (which field ionizes all Rydberg states within a ≈ 60 cm^{-1} window below the ionization threshold). Thus the ponderomotive broadening at the lowest intensity peak (0.9 TW/cm^2 average intensity) is negligible and therefore it is possible to record a three-photon non-resonant ZEKE spectrum of an atom with laser-limited resolution.

The peak maxima are found at 306.4, 306.3 and 306.2 nm, indicating that there is a larger blue-shift with increasing intensity. This corresponds to a ponderomotive shift of the ionization potential of 80, 110 and 140 cm^{-1}, respectively.

If the ZEKE technique should prove useful in time-resolved spectroscopy, the broadening introduced by the ponderomotive shift must be smaller than the effective bandwidth of the laser. This is the case under our conditions at intensities up to 2 TW/cm^2, so we conclude that three-photon ZEKE spectroscopy is a possible detection scheme for atoms in time-resolved experiments. For metal atoms and many molecules, the ionization threshold can be reached with two photons. Under these conditions the required intensity is even lower and the corresponding broadening due to the ponderomotive shift is smaller. We wish to emphasize again that, even under moderate focusing conditions, a laser energies of only a few μJ in 100 fs can introduce a non-negligible broadening of the ZEKE-spectrum. This poses an upper limit on the laser intensity that can be applied in this kind of experiment.

In nanosecond ZEKE experiments the laser intensities are in general much lower but the ultimate resolution is much higher. Recently, a resolution of 0.2 cm^{-1} (0.02 meV) was reported [36]. At intensities on the order of only several GW/cm^2, one introduces a ponderomotive shift of the same order of magnitude as the laser bandwidth, depending on the wavelength. If the resolution of ZEKE spectroscopy should be improved beyond the current limit, one has to ensure that the laser intensity is kept below a wavelength-dependent limit. This is especially important for experiments relying on the two-photon excitation scheme where relatively high intensities must be used in order to achieve a high transition probability.

In conclusion, we have studied the three-photon non-resonant detection of atomic xenon using ZEKE spectroscopy with tunable femtosecond UV pulses. We introduced the idea of ponderomotive shifts in the ZEKE spectrum and demonstrated that it is possible to detect atoms selectively (i.e. as 'recognized' by their ionization potential rather than their charge-to-mass ratio) under conditions where the ponderomotive broadening is smaller than the laser bandwidth. We also implemented a simple model in order to quantify these effects. The results may have implications for the ultimate resolution limits obtainable in ZEKE photoelectron spectroscopy and set limits to intensities in pump–probe experiments using ZEKE photoelectron detection.

Acknowledgement

The authors acknowledge useful discussions with P.B. Corkum and M.Yu. Ivanov. IF would like to thank the Deutsche Forschungsgemeinschaft for a postdoctoral fellowship and AZ acknowledges financial support from CEMAID.

References

[1] A.H. Zewail, Faraday Discussions Chem. Soc. 91 (1991) 1.
[2] A.H. Zewail, in: Femtochemistry: ultrafast dynamics of the chemical bond, (World Scientific, Singapore, 1994), and references therein.
[3] M.H.M. Janssen, M. Dantus, H. Guo and A.H. Zewail, Chem. Phys. Letters 214 (1993) 281.
[4] J.H. Glownia, J. Misewich, R.E. Walkup, M. Kaschke and P.P. Sorokin in: Dye lasers: 25 years, ed. M. Stuke (Springer, Berlin, 1990), and references therein.
[5] S.I. Ionov, G.A. Brucker, C. Jaques, L. Valachovic and C. Wittig, J. Chem. Phys. 97 (1992) 9486.
[6] Y. Chen, L. Hunziker, P. Ludowise and M. Morgen, J. Chem. Phys. 97 (1992) 2149.
[7] M. Dantus, M.H.M. Janssen and A.H. Zewail, Chem. Phys. Letters 181 (1991) 281.
[8] T. Baumert, C. Röttgermann, C. Rothenfusser, R. Thalweiser, V. Weis and G. Gerber, Phys. Rev. Letters 69 (1992) 1512, and references therein.
[9] J. Purnell, S. Wei, S.A. Buzza and A.W. Castleman Jr., J. Phys. Chem. 97 (1993) 12530.
[10] A.P. Baronavski and J.C. Owrutsky, Chem. Phys. Letters 221 (1994) 419.
[11] T. Baumert, B. Bühler, R. Thalweiser and G. Gerber, Phys. Rev. Letters 64 (1990) 733.
[12] J.A. Syage, Chem. Phys. Letters 202 (1993) 227.
[13] K. Müller-Dethlefs, M. Sander and E.W. Schlag, Z. Naturforsch. 39a (1984) 1089.

[14] K. Müller-Dethlefs and E.W. Schlag, Ann. Rev. Phys. Chem. 42 (1991) 109.
[15] J.M. Smith, C. Lakshminarayan and J.L. Knee, J. Chem. Phys. 93 (1990) 4475;
X. Zhang, J.M. Smith and J.L. Knee, J. Chem. Phys. 100 (1994) 2429.
[16] T. Baumert, R. Thalweiser and G. Gerber, Chem. Phys. Letters 209 (1993) 29.
[17] I. Fischer, D.M. Villeneuve, M. Vrakking and A. Stolow, in preparation.
[18] R.G. Tonkyn, J.W. Winniczek and M.G. White, Chem. Phys. Letters 164 (1989) 137.
[19] W. Kong, D. Rodgers and J.W. Hepburn, Chem. Phys. Letters 203 (1993) 497.
[20] H.H. Fielding, T.P. Softley and F. Merkt, Chem. Phys. 155 (1991) 257.
[21] C. Momma, H. Eichmann, A. Tünnerman, P. Simon, G. Marowsky and B. Wellegehausen, Opt. Letters 18 (1993) 1180.
[22] J.H. Glownia, M. Kaschke and P.P. Sorokin, Opt. Letters 17 (1992) 337.
[23] F. Seifert, J. Ringling, F. Noack, V. Petrov and O. Kittelmann, Opt. Letters 19 (1994) 1538.
[24] I. Fischer, A. Strobel, J. Staecker, G. Niedner-Schatteburg, K. Müller-Dethlefs and V.E. Bondybey, J. Chem. Phys. 96 (1992) 7171.
[25] N.B. Delone and V.P. Krainov, Atoms in strong light fields (Springer, Berlin, 1985).
[26] P.H. Bucksbaum, R.R. Freeman, M. Bashkansky and T.J. McIlrath, J. Opt. Soc. Am. B 4 (1987) 760.
[27] R.R. Freeman, P.H. Bucksbaum and T.J. McIlrath, IEEE J. Quantum Electron. 24 (1988) 1461.
[28] A.A. Radzig and B.M. Smirnov, Reference data on atoms, molecules and ions (Springer, Berlin, 1985).
[29] O.L. Landen, M.D. Perry and E.M. Campbell, Phys. Rev. Letters 59 (1987) 2558.
[30] T.R. O'Brian, J.-B. Kim, G. Lan, T.J. McIlrath and T.B. Lucatorto, Phys. Rev. A 49 (1994) R649.
[31] C. Rolland and P.B. Corkum, Opt. Commun. 59 (1986) 64.
[32] P. Dietrich and P.B. Corkum, J. Chem. Phys. 97 (1992) 3187.
[33] J.H. Moore, C.C. Davis and M.A. Coplan, Building scientific apparatus (Addison-Wesley, Redwood City, 1989).
[34] D.M. Villeneuve, I. Fischer, A. Zavriyev and A. Stolow, in preparation.
[35] W.A. Chupka, J. Chem. Phys. 98 (1993) 4520.
[36] R. Lindner, H. Sekiya, B. Beyl and K. Müller-Dethlefs, Angew. Chem. Intern. Ed. Engl. 32 (1993) 603.